Carbohydrate Polymers 79 (2010) 301–305

Contents lists available at ScienceDirect

Carbohydrate Polymers

journal homepage: www.elsevier.com/locate/carbpol

Preparation and properties of glycerol plasticized-starch (GPS)/cellulose nanoparticle (CN) composites

Peter R. Chang [a], Ruijuan Jian [b], Pengwu Zheng [c], Jiugao Yu [b], Xiaofei Ma [b,*]

[a] Agriculture and Agri-Food Canada, Biobased Platforms, 107 Science Place, Saskatoon, SK, S7N 0X2, Canada
[b] School of Science, Tianjin University, Tianjin 300072, China
[c] School of Pharmacy, Jiangxi Science and Technology Normal University, Nanchang, Jiangxi 330013, China

ARTICLE INFO

Article history:
Received 23 July 2009
Received in revised form 28 July 2009
Accepted 3 August 2009
Available online 11 August 2009

Keywords:
Nanocomposites
Starch
Microcrystalline cellulose
Cellulose nanoparticles

ABSTRACT

In this paper, cellulose nanoparticles (CN) were coagulated from a NaOH/urea/H_2O solution of microcrystalline cellulose (MC) using an ethanol/HCl aqueous solution as the precipitant. CN ranged in size from about 50 to 100 nm. Compared to MC, CN formed a new crystalline lattice of cellulose II. The glycerol plasticized-wheat starch (GPS)/CN nanocomposites were prepared using CN as filler in GPS matrix by a casting process. At a low loading level, CN was dispersed evenly in the GPS matrix. The tensile strength increased from 3.15 to 10.98 MPa when CN content went from 0 to 5 wt.%. CN may increase the thermal stability of GPS/CN composites. Moreover, water vapor permeability decreased from 5.75×10^{-10} to 3.43×10^{-10} g m^{-1} s^{-1} Pa^{-1}. The improvements in these properties may be attributed to the good interaction between CN filler and GPS matrix because of the similar polysaccharide structures of cellulose and starch.

1. Introduction

Among naturally biodegradable polymers from renewable resources, starch, which is obtained from a great variety of crops (Angellier, Molina-Boisseau, Dole, & Dufresne, 2006), is probably the most promising material for the production of biodegradable plastics. Starch has been investigated widely for the potential manufacture of products such as water-soluble pouches for detergents and insecticides, flushable liners and bags, and medical delivery systems and devices (Fishman, Coffin, Konstance, & Onwulata, 2000). Native starch exists in a granular structure, which can be processed into continuous phase, i.e., thermoplastic starch (TPS) (Ma & Yu, 2004). However, plasticized starch still exhibits problems such as high water absorption, brittleness (in absence of plasticizer), and the mechanical properties are highly affected by the relative humidity (Kumar & Singh, 2008). One approach to overcome the above-mentioned drawbacks is the addition of the filler as reinforcement for TPS. Many types of filler have been loaded into the plasticized-starch matrix, such as layer silicates, carbon nanotubes, carbon black, metal (platinum, palladium and silver) and metal oxide nanoparticles. Recently, much attention has been paid to preparing totally biodegradable composites with natural polymers and their derivatives (Wu, Wang, Li, Li, & Wang, 2009). The use of polysaccharide nanoparticle fillers has also been studied. Waxy maize starch nanocrystals obtained by hydrolysis of native granules are used as the reinforcing filler in glycerol plasticized-starch (GPS) (Angellier et al., 2006). Another method for the preparation of starch nanoparticles is the delivery of ethanol into starch paste solutions and the synthesis of citrate starch nanoparticles by cross-linking starch nanoparticles with citric acid, which can not be gelatinized in hot water (Ma, Jian, Chang, & Yu, 2008). Cellulose nanocrystallites made by acid hydrolysis of ramie fibers have also acted as the filler in composites with a GPS matrix (Lu, Weng, & Cao, 2006). Nanoparticles from cellulose esters can also be fabricated in *N*,*N*-dimethylacetamide or acetone solution by dialysis or dropping technique (Hornig & Heinze, 2008).

Recently, a new solvent system for cellulose (i.e., NaOH/urea aqueous solution precooled to −10 °C) has been used with which the dissolution of cellulose could easily be achieved (Cai et al., 2007). In this study, cellulose nanoparticles (CN) were prepared from a NaOH/urea/H_2O solution of microcrystalline cellulose (MC) using a novel method of drop-wise addition of an ethanol/HCl aqueous solution as the precipitant. This is a new method to prepare cellulose nanoparticles, which is different from cellulose nanocrystals by acid hydrolysis. During the processing of acid hydrolysis, the amorphous cellulose is degraded by acid hydrolysis, and cellulose nanocrystals in the acicular or rod-like form are prepared. In our method, cellulose components are almost kept in cellulose nanoparticles. This work focuses on processing and characterization of CN and glycerol plasticized-wheat starch (GPS)/CN nanocomposites in terms of size and crystallinity of CN, as well as the morphology, mechanical properties, thermal stability and water vapor permeability of the composites.

* Corresponding author. Tel.: +86 22 27406144; fax: +86 22 27403475.
E-mail address: maxiaofei@tju.edu.cn (X. Ma).

0144-8617/$ - see front matter © 2009 Elsevier Ltd. All rights reserved.
doi:10.1016/j.carbpol.2009.08.007

2. Methods

2.1. Materials

The wheat starch used was Supergell 1203 supplied by ADM-Ogilvy, Canada. Microcrystalline cellulose (MC) was obtained from Tianjin Fine Chemical Institute. Glycerol, NaOH, HCl and urea were purchased from Tianjin Chemical Reagent Factory (Tianjin, China).

2.2. Preparation of cellulose nanoparticles (CN)

MC was dissolved based on the method of Cai and Zhang (2006) with some modifications. An aqueous solution containing NaOH/urea/H_2O, at the ratio of 7:12:81 by weight, was used as a solvent for MC. The solvent was precooled to below −10 °C, and then MC (2 g) was added into the solvent system (200 mL) under vigorous stirring for 30 min at ambient temperature. The solution was centrifuged to remove a small quantity of insoluble MC. A transparent MC solution was obtained. A solution (200 mL) containing 36.5 wt.% HCl aqueous solution/ethanol, at the ratio of 30:170 by volume, was added drop wise to the transparent MC solution, with vigorous stirring. The suspensions were centrifuged at 8000 rpm for 20 min, and the settled CN was washed several times using distilled water to remove the salt and urea. After complete washing, the CN was freeze dried.

2.3. The processing of GPS/CN nanocomposites

CN was dispersed in a solution of distilled water (100 mL) and glycerol (1.5 g) and ultrasonicated for 0.5 h before adding 5 g wheat starch. The CN filler loading level (0, 1, 2, 3, 4 and 5 wt.%) was based on the amount of wheat starch. The mixture was heated at 90 °C for 0.5 h with constant stirring in order to plasticize starch. To obtain the CN/GPS composite films, the mixture was cast into a dish and placed in an air-circulating oven at 50 °C until dry (about 6 h). The composite films were preconditioned in a climate chamber at 25 °C and 50% RH for at least 48 h prior to testing. Water content of the films was about 10 wt.%.

2.4. Transmission electron microscopy (TEM)

A suspension of CN was dropped on a copper grid, air-dried, and examined using a FEI Tecnai G2 F20.

2.5. X-ray diffractometry

MC and CN powders were tightly packed into the sample holder. X-ray diffraction patterns were recorded in the reflection mode in the angular range 5–40° (2θ) at ambient temperature by a BDX 3300 diffractometer, operated at a CuKα wavelength of 1.542 Å. Radiation from the anode, operated at 36 kV and 20 mA, monochromized with a 15 μm nickel foil. The diffractometer was equipped with 1° divergence slit, a 16 mm beam bask, a 0.2 mm receiving slit and a 1° scatter slit. Radiation was detected with a proportional detector.

2.6. Fourier transform infrared (FTIR)

MC and CN were measured at 2 cm^{-1} resolution with a Bio-Rad FTS 3000 IR spectrum scanner.

2.7. Scanning electron microscopy (SEM)

GPS/CN composites were cooled in liquid nitrogen, and then broken. The fracture surfaces of GPS/CN composites were examined using a NanoSEM 430 scanning electron microscope.

2.8. Mechanical testing

The Testometric AX M350-10KN materials testing machine with a crosshead speed of 50 mm/min was used for tensile testing (ISO 1184-1983 standard). The data was averaged for 5–8 specimens.

2.9. Thermogravimetric analysis (TGA)

Thermal properties of CN, GPS and GPS/CN composites were measured on a ZTY-ZP type thermal analyzer. Sample weight varied from 10 to 15 mg. Samples were heated from room temperature to 500 °C at a heating rate of 15 °C/min in a nitrogen atmosphere.

2.10. Water vapor permeability (WVP)

WVP tests were carried out by ASTM method E96 (1996) with some modifications (Yu, Wang, & Ma, 2008). The composite films were cut into circles, sealed over the cell with melted paraffin. The RH in the cell was maintained at 0 using anhydrous calcium chloride in the cell. Each cell was stored in a desiccator containing saturated sodium chloride to provide a constant RH of 100% at 25 °C. WVP was determined by calculating the weight gain of the permeation cell. Changes in the weight of the cell were recorded as a function of time. Slopes were calculated by linear regression (weight change vs. time) and correlation coefficients for all reported data were >0.99. The water vapor transmission rate (WVTR) was defined as the slope (g/s) divided by the transfer area (m^2). After the permeation tests, film thickness was measured and WVP (g Pa^{-1} s^{-1} m^{-1}) was calculated as:

$$\mathrm{WVP} = \frac{\mathrm{WVTR}}{P(R_1 - R_2)} \cdot x$$

where P is the saturation vapor pressure of water (Pa) at the test temperature (25 °C), R_1 is the RH in the desiccator, R_2 is the RH in the permeation cell, and x is the film thickness (m). Under these conditions, the driving force $[P(R_1 - R_2)]$ is 2338 Pa.

3. Results and discussion

3.1. Characterization of CN

According to Mao, Zhang, Cai, Zhou, and Kondo (2008), when an NaOH/urea aqueous solution was precooled to below −10 °C, MC could be dissolved rapidly at room temperature in this cheap and nonpolluting solvent. The low temperature brought out a large inclusion complex associated with cellulose, NaOH, urea, and H_2O clusters which improved the dissolution of cellulose in aqueous solution (Cai et al., 2007). A solution containing 36.5 wt.% HCl aqueous solution/ethanol (at the ratio of 30:170 by volume) was added drop-wise and resulted in the coagulation of MC from the NaOH/urea aqueous solution. The hydrochloric acid component was used to neutralize NaOH in the aqueous solution. As shown in Fig. 1(a), CN was obtained with the size of about 50–100 nm. The interaction of the hydrogen bonds between the coagulated CN and the dissolved cellulose may play an important role in the stability of CN in the suspension (Hornig & Heinze, 2008).

The X-ray diffractograms of MC and CN are shown in Fig. 1(b). MC displayed a typical cellulose I diffraction spectrum with a sharp high peak (200) centered at about 22.4°, two overlapped weaker peaks at about 14.8° and 16.1°, and the weak peak at about 34.4° (Duchemin & Staiger, 2009). CN revealed a different crystalline structure in the X-ray diffractogram. CN was composed of two overlapped peaks at 20.1° and 22.4°, respectively, ascribed to cellulose II (1–10/200) and cellulose I (200) reflection (Gindl,

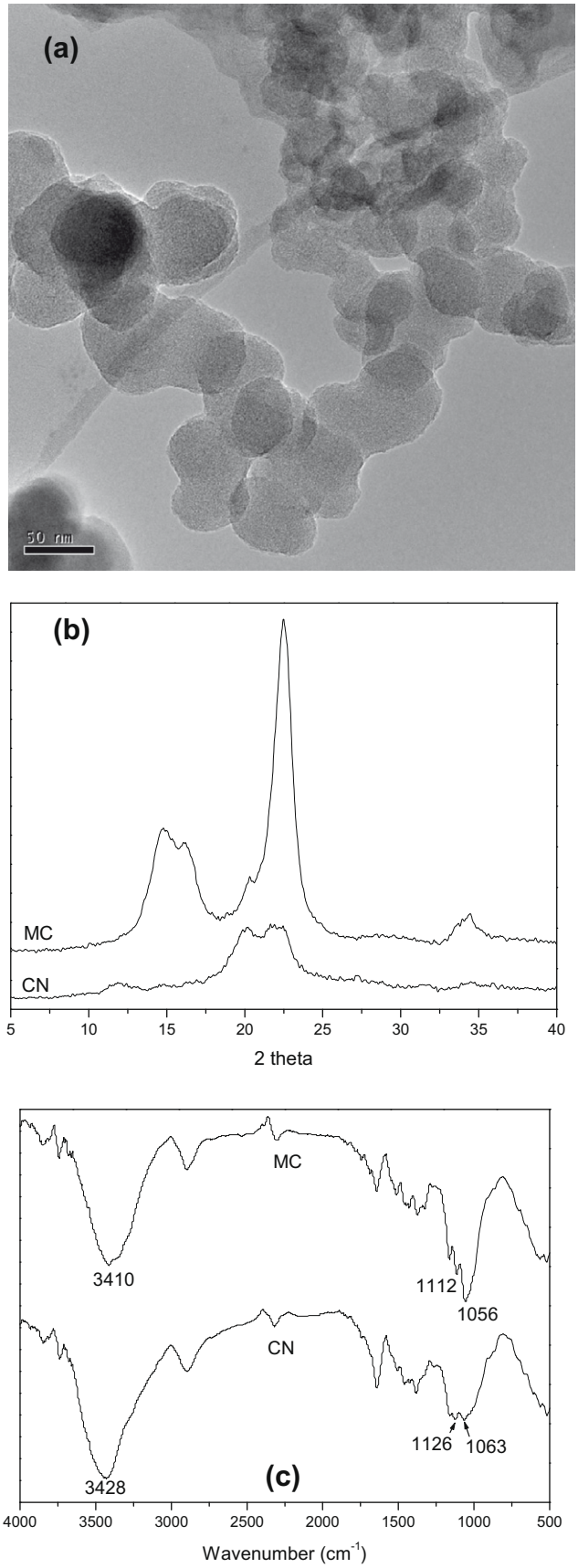

Fig. 1. The characterization of CN particles. (a) TEM of CN; (b) XRD patterns of MC and CN; and (c) FTIR of spectra of MC and CN.

Martinschitz, Boesecke, & Keckes, 2006). The lattice transformation from cellulose I to cellulose II and the decrystallization took place during processing of CN, where swelling and dissolution disrupted the crystalline areas of MC, while the coagulation of CN formed a new crystalline lattice. The dehydrated hydroxide ions of NaOH and urea could easily penetrate the crystal, and undergo a thorough interaction with cellulose for decrystallization (Liu & Hu, 2008). When CN coagulated from the solution, the decreasing NaOH in CN could not prohibit the interaction among cellulose molecules, and new crystalline structure formed.

FTIR measurements were carried out to identify possible interactions among cellulose molecules. In Fig. 1(c), the absorption peak at 3418 cm^{-1} was attributed to the –OH groups of MC, which shifted to higher wavenumbers at around 3428 cm^{-1} in CN. Furthermore, a corresponding effect was shown in the characteristic peaks of MC, where the –C–O bond stretching of –C–O–H group appeared at about 1112 cm^{-1}, and the –C–O bond stretching of –C–O–C group in the anhydroglucose ring appears at about 1056 cm^{-1} (Yu, Yang, Liu, & Ma, 2009). These peaks shifted to higher wavenumbers (around 1126 and 1063 cm^{-1}, respectively) in CN. This shift might be related to the weakening of hydrogen-bond interactions among cellulose molecules (Ma et al., 2008). Both NaOH and urea might interact with the polysaccharide (Ma & Yu, 2004), destroy the original interaction among MC molecules and facilitate the dissolution of MC in the NaOH/urea/H_2O solution. When CN was coagulated from the solution, the interaction among cellulose molecules of CN was weakened.

3.2. Microscopy of the composites

The morphology of composites is a very important characteristic because it ultimately determines many properties of the composites. During the processing of GPS, water and glycerol are well known to disrupt inter- and intramolecular hydrogen bonds, physically breaking up the granules of wheat starch and making the starch become a continuous GPS phase (Ma, Yu, & Wan, 2006). As shown in Fig. 2(a) and (b), SEM micrographs at 10,000× magnification of the fractured surface of composites revealed the distribution of CN in GPS matrix. CN was dispersed evenly in the GPS matrix at low levels (2 wt.%) of CN. At the higher loading of CN (5 wt.%), the dispersion of CN was not uniform in the matrix, and the severe aggregation was recorded in Fig. 2(b).

3.3. Mechanical properties of the composites

Fig. 3 exhibits the effect of CN content on the mechanical properties of GPS/CN composites. As the filler in a GPS matrix, CN had an obvious reinforcement effect. In the processing of GPS/CN composites, the amorphous sections of CN could be easy to swollen and form the interfacial interaction with the matrix. With the increasing CN content, the tensile strength increased, but the elongation at break of the composites decreased. When the CN content varied from 0 to 5 wt.%, the tensile strength increased greatly from 3.15 to 10.98 MPa. This may be ascribed to the good interfacial interaction between CN and the GPS matrix because of similar polysaccharide structures of cellulose and starch. CN could take effects of the physical joints, which could improve the tensile strength, but decrease the flexibility of starch molecules.

3.4. TGA of the composites

Thermogravimetric analysis (TGA) was performed on the composites, where the mass loss due to the volatilization of the

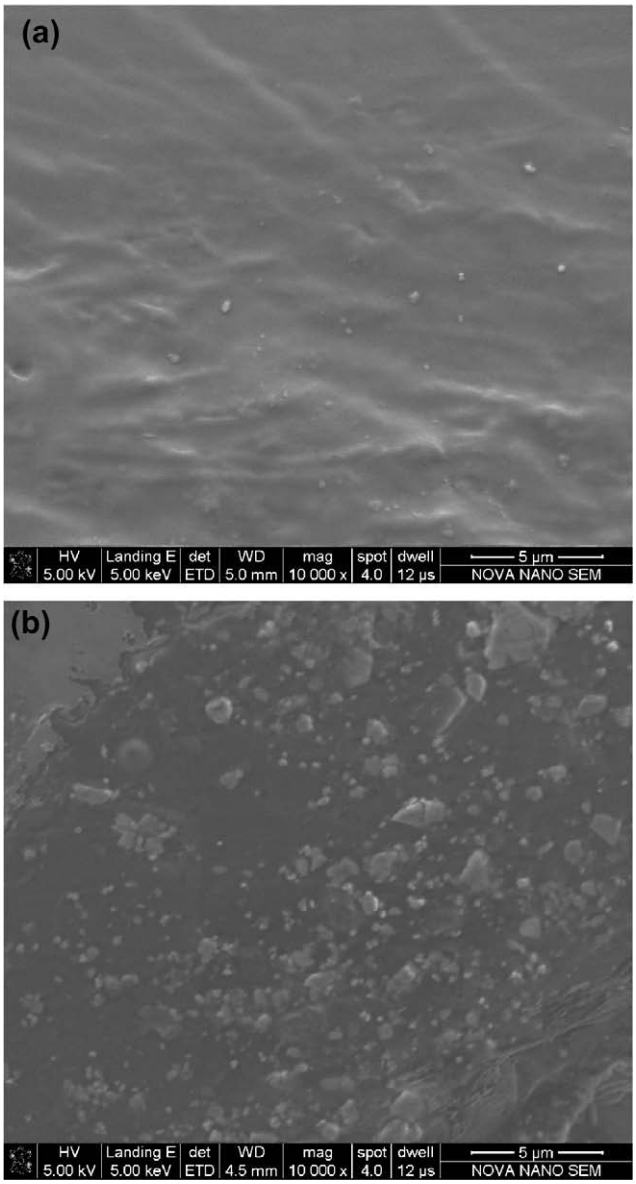

Fig. 2. SEM micrograph of the fragile fractured surface for GPS/CN composites. (a) 2 wt.% CN and (b) 5 wt.% CN.

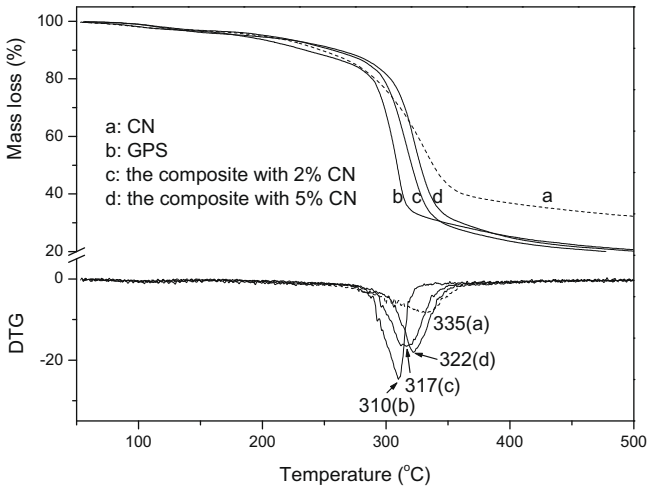

Fig. 4. The thermogravimetric (TG) and derivative thermogravimetric (DTG) curves of CN, GPS, GPS/CN composites.

degradation products was monitored as a function of temperature. The thermogravimetric (TG) and derivative thermogravimetric (DTG) curves of CN, GPS and GPS/CN composites are shown in Fig. 4. The mass loss of GPS and GPS/CN composites before the onset temperature was related to the volatilization of water and glycerol (Ma, Yu, & Ma, 2005). The decomposition temperature, T_{max} was the temperature at the maximum rate of mass loss in TG, i.e., the peak temperature in DTG. The degradation of CN, GPS, GPS/CN (2 and 5 wt.% CN) composites took place at 335 °C, 310 °C, 317 °C and 322 °C, respectively. The introduction of CN may increase thermal stability, which can be ascribed to the better thermal stability of CN as compared to GPS, and to the good interaction between CN and GPS.

3.5. Water vapor permeability of the composite

In food packaging, the film is often required to avoid or at least to decrease moisture transfer between the food and the surrounding atmosphere; water vapor permeability should be as low as possible. As shown in Fig. 5, water vapor easily permeated the GPS film with the highest WVP value at 5.75×10^{-10} g m^{-1} s^{-1} Pa^{-1}. When 1–2 wt.% CN was added into GPS, WVP values decreased noticeably. When more than 3 wt.% CN was added into GPS, the WVP val-

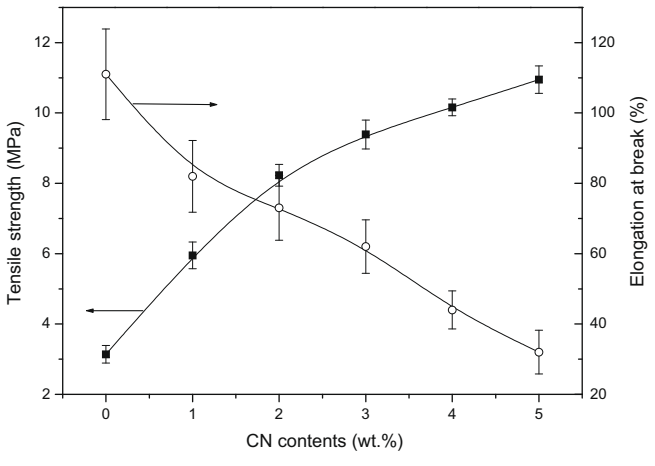

Fig. 3. The effect of CN content on tensile strength and elongation at break of GPS/CN composites.

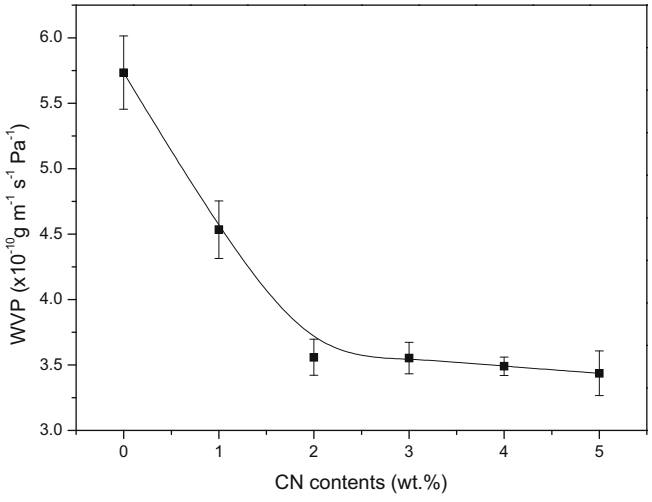

Fig. 5. The effect of CN content on water vapor permeability of composites.

ues gradually decreased. Water resistance of CN was better than that of the GPS matrix. The addition of CN probably introduced a tortuous path for water molecule to pass through (Ma, Chang, Yang, & Yu, 2009). At low contents, CN could disperse well in the GPS matrix (as shown by SEM), which blocked the water vapor. However, excessive CN was easily agglomerated (as shown by SEM), which actually decreased the effective content of CN and facilitated the water vapor permeation.

4. Conclusion

In this study, a simple, novel method was used for the preparation of CN in the size range of about 50–100 nm by drop-wise addition of ethanol/HCl aqueous solution into a NaOH/urea/H_2O solution of MC. The crystalline structure of CN was composed of cellulose I and cellulose II. GPS/CN composites were also fabricated by casting, in which both the filler and the matrix were sourced from natural polysaccharides. CN could be evenly dispersed in the matrix and improve the tensile strength, thermal stability, and water vapor barrier of GPS/CN composites. The effect of the moisture on the properties such as the starch crystalline, thermal stability and water vapor permeability as well as mechanical properties of the composites will be studied further in detail. These polysaccharide composites could be applied in the medical, agricultural, drug release and packaging fields as edible films, disposable or food packaging. In addition, CN could also be used as the filler for other natural polysaccharide (agar, alginate and chitin) matrixes.

References

Angellier, H., Molina-Boisseau, S., Dole, P., & Dufresne, A. (2006). Thermoplastic starch-waxy maize starch nanocrystals nanocomposites. *Biomacromolecules, 7*, 531–539.

Cai, J., & Zhang, L. N. (2006). Unique gelation behavior of cellulose in NaOH/urea aqueous solution. *Biomacromolecules, 7*, 183–189.

Cai, J., Zhang, L., Zhou, J., Qi, H., Chen, H., Kondo, T., et al. (2007). Multifilament fibers based on dissolution of cellulose in NaOH/urea aqueous solution: Structure and properties. *Advanced Materials, 19*, 821–825.

Duchemin, B., & Staiger, M. P. (2009). Treatment of Harakeke fiber for biocomposites. *Journal of Applied Polymer Science, 112*, 2710–2715.

Fishman, M. L., Coffin, D. R., Konstance, R. P., & Onwulata, C. I. (2000). Extrusion of pectin/starch blends plasticized with glycerol. *Carbohydrate Polymers, 41*, 317–325.

Gindl, W., Martinschitz, K. J., Boesecke, P., & Keckes, J. (2006). Structural changes during tensile testing of an all-cellulose composite by in situ synchrotron X-ray diffraction. *Composites Science and Technology, 66*, 2639–2647.

Hornig, S., & Heinze, T. (2008). Efficient approach to design stable water-dispersible nanoparticles of hydrophobic cellulose esters. *Biomacromolecules, 9*, 1487–1492.

Kumar, A. P., & Singh, R. P. (2008). Biocomposites of cellulose reinforced starch: Improvement of properties by photo-induced crosslinking. *Bioresource Technology, 99*, 8803–8809.

Liu, Y. P., & Hu, H. (2008). X-ray diffraction study of bamboo fibers treated with NaOH. *Fibers and Polymers, 9*, 735–739.

Lu, Y. S., Weng, L. H., & Cao, X. D. (2006). Morphological, thermal and mechanical properties of ramie crystallites-reinforced plasticized starch biocomposites. *Carbohydrate Polymers, 63*, 198–204.

Ma, X. F., Chang, P. R., Yang, J. W., & Yu, J. G. (2009). Preparation and properties of glycerol plasticized-pea starch/zinc oxide-starch bionanocomposites. *Carbohydrate Polymers, 75*, 472–478.

Ma, X. F., Jian, R. J., Chang, P. R., & Yu, J. G. (2008). Fabrication and characterization of citric acid-modified starch nanoparticles/plasticized-starch composites. *Biomacromolecules, 9*, 3314–3320.

Ma, X. F., & Yu, J. G. (2004). The plasticizers containing amide groups for thermoplastic starch. *Carbohydrate Polymers, 57*, 197–203.

Ma, X. F., Yu, J. G., & Ma, Y. B. (2005). Urea and formamide as a mixed plasticizer for thermoplastic wheat flour. *Carbohydrate Polymers, 60*, 111–116.

Ma, X. F., Yu, J. G., & Wan, J. J. (2006). Urea and ethanolamine as a mixed plasticizer for thermoplastic starch. *Carbohydrate Polymers, 64*, 267–273.

Mao, Y., Zhang, L., Cai, J., Zhou, J. P., & Kondo, T. (2008). Effects of coagulation conditions on properties of multifilament fibers based on dissolution of cellulose in NaOH/urea aqueous solution. *Industrial and Engineering Chemistry Research, 47*, 8676–8683.

Wu, R. L., Wang, X. L., Li, F., Li, H. Z., & Wang, Y. Z. (2009). Green composite films prepared from cellulose, starch and lignin in room-temperature ionic liquid. *Bioresource Technology, 100*, 2569–2574.

Yu, J. G., Wang, N., & Ma, X. F. (2008). Fabrication and characterization of poly(lactic acid)/acetyl tributyl citrate/carbon black as conductive polymer composites. *Biomacromolecules, 9*, 1050–1057.

Yu, J. G., Yang, J. W., Liu, B. X., & Ma, X. F. (2009). Preparation and characterization of glycerol plasticized-pea starch/ZnO–carboxymethylcellulose sodium nanocomposites. *Bioresource Technology, 100*, 2832–2841.